

ACCEPTED MANUSCRIPT

Towards the use of breath for detecting mycobacterial infection: a case study in a Murine model

To cite this article before publication: Flavio Antonio Franchina *et al* 2017 *J. Breath Res.* in press <https://doi.org/10.1088/1752-7163/aaa016>

Manuscript version: Accepted Manuscript

Accepted Manuscript is “the version of the article accepted for publication including all changes made as a result of the peer review process, and which may also include the addition to the article by IOP Publishing of a header, an article ID, a cover sheet and/or an ‘Accepted Manuscript’ watermark, but excluding any other editing, typesetting or other changes made by IOP Publishing and/or its licensors”

This Accepted Manuscript is © 2017 IOP Publishing Ltd.

During the embargo period (the 12 month period from the publication of the Version of Record of this article), the Accepted Manuscript is fully protected by copyright and cannot be reused or reposted elsewhere.

As the Version of Record of this article is going to be / has been published on a subscription basis, this Accepted Manuscript is available for reuse under a CC BY-NC-ND 3.0 licence after the 12 month embargo period.

After the embargo period, everyone is permitted to use copy and redistribute this article for non-commercial purposes only, provided that they adhere to all the terms of the licence <https://creativecommons.org/licenses/by-nc-nd/3.0>

Although reasonable endeavours have been taken to obtain all necessary permissions from third parties to include their copyrighted content within this article, their full citation and copyright line may not be present in this Accepted Manuscript version. Before using any content from this article, please refer to the Version of Record on IOPscience once published for full citation and copyright details, as permissions will likely be required. All third party content is fully copyright protected, unless specifically stated otherwise in the figure caption in the Version of Record.

View the [article online](#) for updates and enhancements.

1
2
3 **1 TOWARDS THE USE OF BREATH FOR DETECTING MYCOBACTERIAL**
4
5 **2 INFECTION: A CASE STUDY IN A MURINE MODEL**
6
7
8
9

10 4 Flavio A. Franchina¹, Theodore R. Mellors¹, Minara Aliyeva², Jeff Wagner³, Nirav Daphtary²
11
12 5 Lennart K.A. Lundblad², Sarah M. Fortune³, Eric J. Rubin³, and Jane E. Hill^{1,*}
13
14
15
16

17 7 ¹*School of Engineering at Dartmouth College, 14 Engineering Drive, 03755 Hanover (NH),*

18
19 8 *United States*

20
21 9 ²*University of Vermont, College of Medicine, 149 Beaumont Ave., 05405 Burlington (VT),*

22
23
24 10 *United States*

25
26 11 ³*Harvard School of Public Health, Department of Immunology and Infectious Diseases, 02115*

27
28 12 *Boston (MA), United States*
29
30
31
32

33 14 Manuscript prepared for submission as an original research article to **Journal of Breath**
34
35 15 **Research**
36
37
38
39

40 17 *Corresponding author. *E-mail address:* jane.e.hill@dartmouth.edu
41
42
43
44
45
46
47
48
49
50
51
52
53
54
55
56
57
58
59
60

1
2
3 **24 Abstract**
4

5
6 **25** In the present research, the potential of breath analysis by comprehensive two-dimensional gas
7
8 **26** chromatography coupled to mass spectrometry (GC×GC-MS) was investigated for the
9
10 **27** discrimination between healthy and infected mice. A pilot study employing a total of 16 animals
11
12 **28** was used to develop a method for breath analysis in a murine model for studying MTBC
13
14 **29** (*Mycobacterium tuberculosis* complex) using the *M. bovis* BCG (Bacillus Calmette-Guérin).
15
16
17 **30** Breath was collected in Tedlar bags and concentrated onto thermal desorption tubes for the
18
19 **31** subsequent analysis by GC×GC-MS. Immunological test and bacterial cell count in
20
21 **32** bronchoalveolar lavage fluid and mice lung homogenate confirmed the presence of bacteria in
22
23 **33** the infected group. From the GC×GC-MS analysis, 23 molecules were found to mainly drive the
24
25 **34** separation between control and infected mice and their tentative identification is provided.
26
27
28 **35** This study shows that the overall used methodology is able to differentiate breath between
29
30 **36** healthy and infected animals and the information herein can be used to further develop the
31
32 **37** mouse breath model to study MTBC pathogenesis, evaluate pre-clinical drug regimen efficacy,
33
34 **38** and to further develop the concept of breath-based diagnostics.
35
36
37
38
39
40
41
42
43
44
45
46

45 **Keywords:** *Mycobacterium tuberculosis* complex; breath analysis; comprehensive two-
46 dimensional gas chromatography; mass spectrometry; volatile metabolites;

47 1. Introduction

48 Since the beginning of recorded history, breath has been used to gain insight into disease
49 pathogenesis. For example, in the Ancient Greece, Hippocrates recognized the diagnostic
50 usefulness of breath, describing *fetor oris* and *fetor hepaticus* (bad breath due to putrid humors in
51 the stomach and by liver failure, respectively) in his treatise on breath aroma and disease [1].

52 In the contemporary era, Linus Pauling was the first to demonstrate that human breath was
53 composed of many molecules, and not only the classic gases nitrogen, oxygen, carbon dioxide
54 and water vapor. Pauling reported the presence of 250 molecules in exhaled breath using gas
55 chromatography with a flame ionization detector (GC-FID) [2].

56 Generally, a breath sample is easy to obtain (non-invasive) and contains thousands of molecules,
57 some of which have the potential for use in diagnostic applications [3,4]. To-date, breath analysis
58 has been used to track or diagnose a variety of diseases in humans; for example, in metabolic
59 disorders, monitoring specific metabolites (short chain fatty acids) during a glucose challenge in
60 diabetic patients [5], in lung-related diseases, such as cancer [6], chronic obstructive pulmonary
61 disease [7], and bacterial pneumonias infections (*e.g.* caused by *Staphylococcus aureus*,
62 *Escherichia coli*, and *Candida spp*) [8].

63 Infectious diseases are the major cause of death in many countries, and earlier diagnosis may
64 result in the earlier initiation of appropriate antimicrobial therapy, as well as limit disease
65 transmission, thus decreasing both morbidity and mortality.

66 The traditional microbiological diagnostic tests are time-consuming, such as for the common
67 bacterial pathogen *S. aureus*, the gold standard culture approach can take 2-4 days, and even
68 longer (up to 3-6 weeks) for slow-growing bacteria (*i.e.*, *Mycobacterium tuberculosis* complex
69 (MTBC) organisms) [9].

1
2
3 70 These organisms belonging to MTBC are a group of genetically-related mycobacteria which can
4
5 71 cause tuberculosis, which is responsible for considerable morbidity and mortality worldwide,
6
7
8 72 with 10.5 million new cases and 1.5 million deaths in 2015 [10].
9

10 73 The MTBC comprises *M. tuberculosis*, *M. bovis*, *M. africanum*, *M. caprae*, *M. microti*, *M.*
11
12 74 *canettii*, *M. pinnipedii*, *M. orygis*, and *M. mungi* and the predominant infection location for these
13
14 75 organisms is in the lungs, even though infections at other bodily sites can occur [11].
15

16
17 76 Breath molecules have been proposed as a way to diagnose MTBC infections and could also be
18
19 77 used to track patient treatment response. Seven published studies focusing on *M. tuberculosis*
20
21 78 lung infection in humans have analyzed breath collected from over 300 confirmed tuberculosis-
22
23 79 positive individuals, and over 1000 patients overall [12–18]. Of note, from these seven studies,
24
25 80 only one molecule (tridecane) is shared between two studies and reported as a tuberculosis-
26
27 81 associated biomarker. This lack of biomarker consistency is likely due to a series of factors,
28
29 82 including the complexity, co-morbidity and metabolic heterogeneity within the human
30
31 83 population, as well as the use of different analytical approaches and differences in study design.
32
33

34
35 84 In animals, limited studies have been conducted on breath from individuals infected with MTBC.
36
37 85 Two studies on bovine breath involved a total of 25 infected animals [19,20] and one non-human
38
39 86 primate study involving 5 infected animals [21], showed that healthy and diseased animals could
40
41 87 be distinguished using volatile molecules detectable in breath.
42
43

44 88 Few studies have attempted to link the breath volatile metabolites to disease pathogenesis. To-
45
46 89 date, only one study has sought to link mycobacterial metabolism and *in vivo* pathogenesis via
47
48 90 human breath [12]. As it is complicated to look for causative links in a heterogeneous study
49
50 91 population, such as humans, animal models are generally employed as a first step.
51
52
53
54
55
56
57
58
59
60

1
2
3 92 Among these, the murine model is the most commonly used animal model for MTBC infections,
4
5 93 due to ease of manipulation and housing, availability of inbred strains or mutants, cost, and
6
7 94 genetically-altered strains. To that end, the mouse has been used extensively to model various
8
9 95 aspects of MTBC infections, employing mutant strains, immune response, assessing drug
10
11 96 efficacy, and new vaccines evaluation [22].
12
13

14 97 In the present research, a pilot study employing 16 mice was used to develop a method for breath
15
16 98 analysis in a murine model for studying MTBC using *M. bovis* BCG (Bacillus Calmette-Guérin),
17
18 99 a Biosafety Level 2 organism. Breath was collected in Tedlar bags from anesthetized, intubated
19
20
21 100 mice and concentrated onto thermal desorption tubes for the subsequent analysis by
22
23 101 comprehensive 2D gas chromatography coupled to mass spectrometry (GC×GC-MS) [23]. The
24
25 102 presence of infection was confirmed with immunological test and bacterial cell count in
26
27 103 bronchoalveolar lavage fluid and mice lung homogenate, respectively. A tentative identification
28
29 104 of the molecules in breath (sampled at two distinct sampling points) driving the separation
30
31 105 between control and infected mice is provided. The information obtained in this study can be
32
33 106 used to further develop the mouse breath model for MTBC lung infections.
34
35
36
37

38 107

39 108 **2.0 Materials and Methods**

40 109 ***2.1 Bacterial strain, growth and inoculant preparation***

41
42 110 The *M. bovis* BCG substrain was obtained from the Harvard T.H. Chan School of Public Health
43
44 111 (Boston, MA), and it was cultured aerobically (21 days; 37°C under agitation) in 20 mL
45
46 112 Middlebrook 7H9 (BD Diagnostics, Franklin Lakes, NJ, USA), supplemented with ADC
47
48 113 enrichment (BD Diagnostics), 0.05% Tween 20 and 0.2% glycerol, before bacteria were
49
50
51 114 inoculated into the mice airways. For inoculation in murine lung, the cultures were washed 3
52
53
54
55
56
57
58
59
60

1
2
3 115 times and resuspended in phosphate-buffered saline (PBS, pH = 7.4) to the desired final
4
5 116 concentration.
6
7

8 117

9 10 118 **2.2 Mice and infection route**

11
12 119 All mice were housed in the Association for Assessment and Accreditation of Laboratory
13
14 120 Animal Care (AAALAC)-accredited animal facility at the University of Vermont (Burlington,
15
16 121 VT). The protocol for animal infection and respiratory physiology measurements was approved
17
18 122 by the Institutional Animal Care and Use Committee, in accordance with AAALAC guidelines.
19
20 123 Male C57BL/6J mice (10 – 12 week-old) were purchased from The Jackson Laboratories (Bar
21
22 124 Harbor, ME). Mice were exposed to 50 μ L inoculum in the 10^5 - 10^6 CFU (colony-forming unit)
23
24 125 range of *M. bovis* BCG cell via oropharyngeal aspiration, as previously reported [24], and breath
25
26 126 was collected at either 24h ($n = 4$ per group) and 48h ($n = 4$ per group) post-inoculation. The
27
28
29 127 control group were inoculated with 50 μ L of PBS and treated identically. A total of 16 mice were
30
31
32 128 used.
33
34

35 129

36 130

37 38 39 131 **2.3 Exhaled breath collection**

40
41
42 132 Twenty-four and forty-eight hours after the *M. bovis* BCG or PBS instillation, mice were
43
44 133 anesthetized with pentobarbital and their tracheas cannulated. The mice were placed on the
45
46 134 ventilator (flexiVent, SCIREQ, Montreal, QC, Canada). Breath from the ventilator was collected
47
48 135 in 1L Tedlar bags (SKC, Eighty Four, PA) at 200 breaths/min with a positive end expiratory
49
50
51 136 pressure (PEEP) of 3 cm H₂O for 30 – 40 min [24]. Room air samples ($n = 16$) were collected by
52
53
54 137 attaching the Tedlar bag to the ventilator in absence of mouse. Only new Tedlar bags after the
55
56
57
58
59
60

1
2
3 138 conditioning step were used for collecting breath and room air. The conditioning step consisted
4
5 139 of flushing the bags with UHP nitrogen gas and condition them in an incubator at 37°C for 30
6
7 140 minutes. This process was repeated 3 times. After bag filling, the breath or room air volatile
8
9 141 molecules were concentrated by drawing the content of the Tedlar bag onto thermal desorption
10
11 142 tubes packed with Carboxen 1000 (Supelco, Bellefonte, PA) via
12
13 143 a vacuum pump, at an average flow rate of 170 mL/min. The sampling flow rate was measured
14
15 144 during each tube loading by means of a flowmeter and the total drawing time was adjusted to
16
17 145 have a constant final volume of *circa* 1 L.

18
19
20
21 146 The loading onto thermal desorption tubes was completed within five min of breath collection.
22
23 147 Tubes were stored at 4°C and analyzed in the GC×GC-MS within two weeks of collection.
24
25

26 148

27 28 149 ***2.4 Collection and analysis of bronchoalveolar lavage fluid and lung tissue***

29
30
31 150 After the breath collection, 1 mL of room temperate PBS was instilled into the lungs via the
32
33 151 tracheal cannula and then withdrawn. The BALF (bronchoalveolar lavage fluid) was centrifuged
34
35 152 and the supernatant collected. The remaining cell pellet was resuspended in 400 µl of PBS and an
36
37 153 aliquot (150 µl) of the bronchoalveolar lavage was run on the Guava easyCyte 6HT-2L benchtop
38
39 154 flow cytometer. Cell counts were calculated using two parameters, the (A) concentration
40
41 155 (particles/ml) and (B) cell percentage gated according to particle size (forward scatter, FSC) and
42
43 156 granularity (side scatter, SSC) to exclude RBCs (red blood cells) and debris. The following
44
45 157 calculation was applied: $A \cdot (B \cdot 0.01) \cdot 0.4 =$ absolute total cell count. The cell concentration of the
46
47 158 BALF cells was adjusted to 200 µl⁻¹ and 100 µl was loaded into Cytospin funnels and spun onto
48
49 159 glass slides at 600 RPM for 6 minutes. Following drying the cells were stained using a HEMA 3
50
51 160 kit (Fisher Scientific); first fixated in a methanol solution for 2 minutes then stained with Eosin
52
53
54
55
56
57
58
59
60

1
2
3 161 Y for 2 minutes, and finally in Azure A and methylene blue for 30 seconds. The cells were
4
5 162 differentiated by counting 300 cells/slide differentiating into eosinophils, neutrophils,
6
7 163 macrophages, and lymphocytes.
8
9

10 164 After the bronchoalveolar lavage was obtained lungs were harvested and homogenized. The
11
12 165 excised lungs were trimmed free from adjacent tissue and the lung lobes placed in sterile
13
14 166 gentleMACS M tubes (Miltenyi Biotec, Auburn, CA) with 3 ml of PBS. The lungs were
15
16 167 homogenized by running the RNA_01 program on a gentleMACS dissociator. Lung bacterial
17
18 168 cell counts were obtained after 21 days at 37°C by plating an aliquot of the lung homogenate on
19
20 169 7H10 Middlebrook agar plates supplemented with OADC (BD Diagnostics).
21
22

23
24 170 The bronchoalveolar lavage fluid was centrifuged, the resulting pellet was cultured neat (no
25
26 171 dilutions), and the presence of visible colonies was assessed after three weeks as an additional
27
28 172 confirmatory test for the presence of bacterial cells in the lungs at the moment of breath
29
30 173 collection. Bronchoalveolar lavage fluid cell differentiation and cell count were performed in
31
32 174 triplicate.
33
34

35 175

36 176 *2.5 Analytical instrumentation and statistical analysis*

37
38 177 Thermal desorption tubes were analyzed in a Pegasus 4D (LECO Corporation, St. Joseph, MI)
39
40 178 GC×GC time-of-flight (TOF) MS instrument with an Agilent 7890 GC equipped with a TDU,
41
42 179 CIS and an MPS auto sampler (Gerstel, Linthicum Heights, MD). Details of the sample
43
44 180 desorption, chromatography and mass spectrometry experimental conditions are summarized in
45
46 181 **Table 1.** Data acquisition and analysis were performed using ChromaTOF software, version 4.50
47
48 182 (LECO Corp.).
49
50
51
52
53
54
55
56
57
58
59
60

1
2
3 183 Chromatographic data were processed and aligned using ChromaTOF. For peak identification, a
4
5 184 signal-to-noise (S/N) cutoff was set at 20, and resulting peaks were identified by a forward
6
7
8 185 search of the NIST 2011 library. For tentative peak identification, a forward match score of 800
9
10 186 (of 1000) was required. For the alignment of peaks across chromatograms, maximum first and
11
12 187 second-dimension retention time deviations were set at 6s and 0.1s, respectively, and the inter-
13
14 188 chromatogram spectral match threshold was set at 700.

15
16
17 189 All statistical analyses were performed using R (version 3.3.0). Prior to statistical analyses,
18
19 190 samples were normalized using probabilistic quotient normalization [25]. After the manual
20
21 191 removal of artifacts (see supplementary Table S1), a further feature reduction step was
22
23 192 performed, removing features present in less than 50% of the chromatograms in the *M. bovis*
24
25 193 BCG infected, PBS control mice or room air groups. Random forest was then applied for the
26
27 194 selection of features that discriminate between these three groups [26]. Features were selected as
28
29 195 discriminatory if they were ranked in the top 100 in 100/100 random forest iterations of 1000
30
31 196 trees, based on their mean decrease in impurity. Principal component analysis (PCA) was used to
32
33 197 visualize the variance between samples when looking at the selected discriminatory features
34
35 198 [26]. Centroid analysis was used to visualize the center of the *M. bovis* BCG, PBS control, and
36
37 199 room air clusters based on their principal component (PC) scores [26]. The significance of the
38
39 200 compounds was tested by means of the Mann-Whitney U test.
40
41
42
43
44
45
46
47
48
49
50
51
52
53
54
55
56
57
58
59
60

206 **Table 1.** Summary of GC×GC-TOFMS experimental conditions.

Thermal desorption tubes and desorption process	
Sorbent material	Carbopack Y, Carbopack X, Carboxen 1000
Solvent venting time (TDU temperature; flow rate)	10 min (30°C; 60 ml/min)
Thermal desorption time (TDU temperature; flow rate)	5 min (330°C; 60 ml/min)
Cryofocusing time (CIS temperature)	5 min (-120°C)
Sample desorption time, CIS temperature, injection mode	180 s, 330 °C, splitless
GC×GC	
D1 column (L × ID × d _i)	Rxi-624Sil (60 m × 0.25 mm × 1.4 μm)
D2 column (L × ID × d _i)	Stabilwax (1 m × 0.25 mm × 0.5 μm)
D1 oven temperature	35 to 235°C at 3.5 °C/min
D2 oven and modulator temperature	+ 5°C and + 25 °C relative to D1 oven temp
Modulation period (hot/cold jet)	2.5 s total (alternating 0.85 s/0.4 s hot/cold)
Carrier gas (flow rate)	Helium (2 mL/min)
Transfer line temperature	260 °C
MS	
Acquisition mass range	30 - 400 <i>m/z</i>
Acquisition frequency	200 Hz
Ion source temperature	200 °C

207

208 **3.0 Results and Discussion**209 **3.1 Murine infection confirmation**

210 To verify the presence of bacteria at the time of breath sampling, cell count was obtained after
 211 plating homogenized lungs and bronchoalveolar lavage fluid. For mice infected with *M. bovis*
 212 BCG, bacterial counts from homogenized lungs at the time of breath sampling ranged between 1
 213 $\times 10^4$ and 1×10^6 CFU/mouse and were not statistically different ($p = 0.35$) between 24 h and 48
 214 h sampling points. Mice inoculated with the phosphate-buffer saline did not yield any bacterial
 215 colonies from either lung homogenate or bronchoalveolar lavage fluid (**Supplementary Figure**
 216 **S1**).

217 Additionally, bronchoalveolar lavage fluid from mice inoculated with *M. bovis* BCG cultured
 218 positive while mice inoculated with PBS cultured negative, confirming the homogenate results.

219 To further confirm infection status, host immune cell differentiation in the bronchoalveolar
 220 lavage fluid was measured. No eosinophil and lymphocytes were found in any of the mice since
 221 they are commonly the predominant cells observed during allergic states [27] and thus no to be
 222 expected during bacterial infection. An average (\pm SD) of $2.2 \pm 0.8 \times 10^5$ neutrophils were

measured in bronchoalveolar lavage fluid of animals exposed to *M. bovis* BCG, which was significantly greater ($p = 0.00094$) than the PBS control group, where none were detected (see **Figure 1**). This is in agreement with other murine studies which highlighted neutrophil influx in the lungs during early active bacterial infections [28,29], including with *M. bovis* BCG after intranasal infection [30]. No significant differences in neutrophil number ($p = 0.88$) were observed between the two harvesting time points.

The average concentration of macrophages in the bronchoalveolar lavage fluid were $1.3 \pm 0.9 \times 10^5$ and $5 \pm 1.4 \times 10^4$ cells for the mice inoculated with BCG and PBS, respectively, and was significantly different ($p = 0.04$) between the two groups (**Figure 1**). No significant difference in macrophages cell number ($p = 0.8$) between the two harvesting time points was observed. The macrophage concentration, both in the infected and control groups, is in agreement with the literature [29,31,32]. Taken together, these biological assays indicate successful infection for the mice inoculated with *M. bovis* BCG.

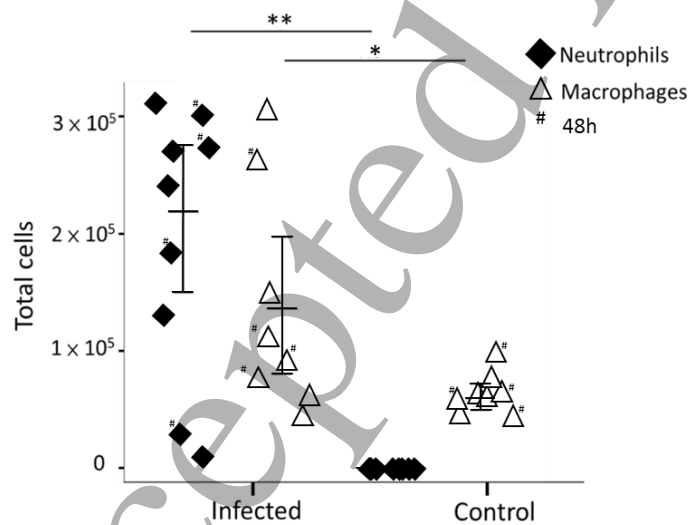


Figure 1. Concentration of neutrophils (solid diamonds) and macrophages (open triangles) in bronchoalveolar lavage fluid collected from infected and control mice ($n = 8$ per group) at either 24 h or 48 h post-inoculation. No eosinophil and lymphocytes are plotted since they were not

240 present. Error bars represent the 95% interval confidence and significance values were calculated
241 applying the Mann-Whitney significance U-test ($*p < 0.05$; $**p < 0.01$).

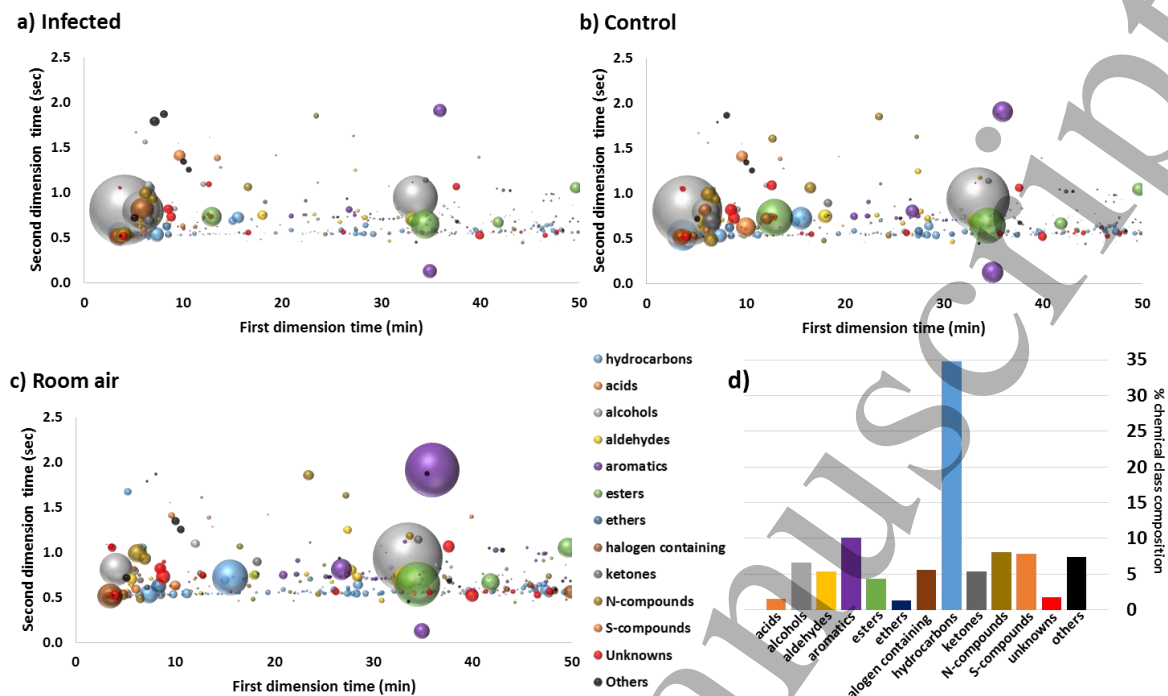
243 **3.2. Breathprint of control and infected mice**

244 Breath from mice inoculated with *M. bovis* BCG and PBS ($n = 8$ per group), as well as room air
245 samples ($n = 16$), were analyzed using GC×GC-TOFMS. The flowchart of the data reduction
246 steps adopted in the current study is shown in **Supplementary Figure S2**.

247 Across the 32 samples, approximately 1600 peaks were detected. In a preliminary data cleaning
248 step, 300 peaks were removed based on mass spectrum [33] and presence in all samples (both
249 room air and breath were collected in Tedlar bags). A spectral similarity to known environmental
250 contaminants or artifacts coming from the Tedlar bags (*e.g.*, phenol and N,N-dimethylacetamide)
251 or column bleed (*e.g.*, siloxane or silyl derivatives), in addition to their persistent presence in all
252 the chromatograms, drove the exclusion criteria (for a more detailed list of excluded features see
253 Supplementary Table S1).

254 In order to direct data analysis to consistently detected peaks, those present in more than 50% of
255 samples from each group (infected, control, and room air) were considered for further analysis,
256 resulting in 604 features.

257 Bubble plots representing the two-dimensional GC separation obtained from the infected and
258 control mouse breath, and the room air samples are reported in **Figure 2a-c**, respectively. Each
259 bubble represents a chromatographic peak and bubble position is given by the retention time
260 coordinates of the peak (*i.e.*, first and second dimension retention time). The size of the bubble
261 corresponds to the peak area calculated from the deconvoluted MS signal.



262
 263 **Figure 2a-d.** Bubble plot of the GC×GC chromatograms of breath from a) mice infected with
 264 *M. bovis* BCG, b) mice inoculated with PBS, and c) room air samples. Each bubble represents a
 265 detected peak and the size is proportional to the average area across chromatograms belonging to
 266 that sample group. Only features (604) present in 50% of the samples from single class are
 267 plotted. d) Chemical class relative abundance based on number of identified compounds, not on
 268 their relative concentration.

269
 270 The profile of the 604 features was found to have a moderate correlation among the samples
 271 analyzed, with a Spearman's rank correlation of 0.53, 0.5, and 0.52 for the mice treated with
 272 *M. bovis* BCG, PBS, and room air samples, respectively [34].

273 Most of the 604 peaks were assigned chemical classification based on their mass spectral
 274 similarities (≥ 800) to the NIST 2011 library (**Figure 2a-d**). A wide range of chemical classes
 275 was found (*i.e.*, carboxylic acids, alcohols, aldehydes, aromatic, halogen-containing, N-
 276 containing, S-containing compounds, ethers, esters, ketones) with the hydrocarbons being the
 277 most commonly present chemical class (34%) (**Figure 2d**). The other remaining chemical

1
2
3 278 classes ranged from 2-10 % of breath composition. These classes have been previously reported
4
5 279 in the breath of animals and humans, with the hydrocarbons being the most abundant [4,12–21].
6
7

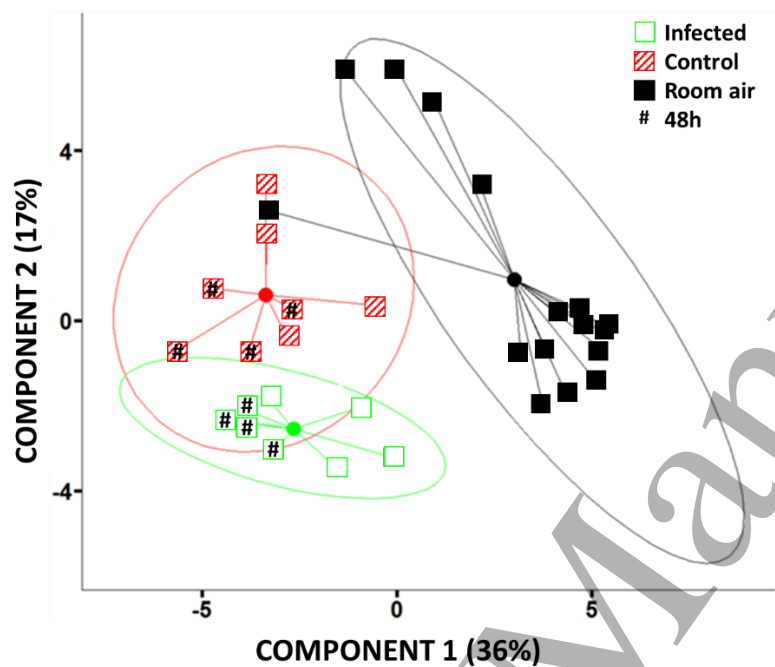
8 280

9 281 **3.3. Selected molecules in breath for infected and control mice discrimination**

10 282 From the 604 detected breath molecules, 23 features were selected by random forest that
11
12 283 discriminated between mice infected with *M. bovis* BCG, mice inoculated with PBS, and room
13
14 284 air samples. When considering these 23 selected features, the correlation between breath samples
15
16 285 of the same class is highly correlated, with a Spearman's rank correlation of 0.7, 0.57, and 0.55
17
18 286 for the mice treated with *M. bovis* BCG, PBS, and room air samples, respectively [34]. The
19
20 287 lower correlation between room air samples when considering these 23 selected features is
21
22 288 possibly due to variations in room air composition on different days of sampling.
23
24
25
26
27

28 289 Principal components scores were used to visualize variance between these sample types (**Figure**
29
30 290 **3**). The first two components explain 53% of the variance between the three group types. Data
31
32 291 centroids (**Figure 3**, circles) illustrate the average position on component 1 and component 2 of
33
34 292 all the samples for each group. The Euclidean distance between breath (infected and control
35
36 293 mice) and room air was found to be 1.9 times greater than the distance between BCG and PBS
37
38 294 clusters. Although differences in profile are observed between these three groups when
39
40 295 considering the 23 selected molecules, the small sample size of the present study prevented
41
42 296 external validation of these preliminary findings. Therefore, future studies are necessary to
43
44 297 evaluate the reproducibility of these identified biomarkers. Both the 24 h and 48 h breath
45
46 298 samples cluster within their respective groups, suggesting that the discriminatory features of the
47
48 299 breath profile are maintained across the two sampling points. One room air sample is
49
50 300 misclassified, falling within the control group sample projections. All the room air samples
51
52
53
54
55
56
57
58
59
60

1
2
3 301 collected from the same day cluster with their respective and expected group, therefore, the
4
5 302 reason for this misclassification is unclear.
6
7
8 303



9
10
11
12
13
14
15
16
17
18
19
20
21
22
23
24
25
26
27
28
29
30
31 304
32
33 305 **Figure 3.** Centroid analysis using principal component scores of the *M. bovis* BCG infected mice
34 306 (red striped square), PBS-inoculated mice (green empty square) and the room air (black solid
35 307 square), considering the 23 discriminatory features. Ellipses represent the 95% confidence
36 308 interval for each class.
37
38
39
40 309

41
42 310 Tentative identifications were provided for all 23 features based only on mass spectral matches
43
44 311 to the NIST 2011 library (≥ 800) and are reported in **Table 2**.

45
46 312 These molecules belong to eight different chemical classes (nine hydrocarbons, four aldehydes,
47
48
49 313 one N-containing and two S-containing compounds, two alcohols, one ester, two aromatics, and
50
51 314 two ketones). Two of these molecules (2-methyl-(E)-2-butenal and 2-ethyl-3-methylbutanal)
52
53 315 were exclusively detected in breath (*i.e.*, not detected in any room air samples) while 21 were
54
55
56 316 present in all samples but at different concentrations. It should be pointed out that even if MS
57
58
59
60

1
2
3 317 spectra library comparison commonly used in GC-MS applications for peak identification, the
4
5 318 final confirmation should be assessed by injecting analytical standards.
6
7
8 319 Based on principal components loading scores, the molecules that mainly drive the separation
9
10 320 between infected and control mice were: 4-methyldecane, 2,4,4-trimethyl-1-pentene, butanal, 3-
11
12 321 oxo cyclopenten-1-yl-(2E)-penta-2,4-dienoate, acetaldehyde, decyl-cyclohexane, acetone and
13
14 322 3,4-diethyl-2-hexane (**Supplementary Figure S3**). Only decyl-cyclohexane was significantly
15
16 323 more abundant in infected mice compared with the control mice treated with PBS ($p < 0.05$).
17
18
19 324 These molecules were detected in breath of both infected and control mice, but they were
20
21 325 differentially abundant (**Table 2**). A connection between these molecules and specific metabolic
22
23 326 pathways has yet to be determined.
24
25
26 327 To the best of the authors' knowledge, this study represents the first time breath has been
27
28 328 evaluated from mice infected with any MTBC organisms. In considering previous studies of
29
30 329 exhaled breath in the context of mycobacteria infection, there are few, and they are limited to
31
32 330 cows [19,20], non-human primates [21], and humans [12–18]. Beyond the use of different
33
34 331 models, there are some important differences in the studies, including the I) *Mycobacterium*
35
36 332 species and strain used (*M. bovis* in cows, *M. tuberculosis* Erdman in non-human primates,
37
38 333 unknowns *M. tuberculosis* strain(s) in humans, vs. *M. bovis* BCG in the present study), II)
39
40 334 longevity of infection (3 months (cows), 1-2 months (non-human primates), unknown (humans),
41
42 335 vs. 24-48 h in the present study), and III) breath volume collected (1.5L (cows and non-human
43
44 336 primates), 1L (humans), vs. 1L in the present study). In addition, each study used different
45
46 337 sorbent phases to concentrate and store breath. One study [21] used the same analytical
47
48 338 technique as this study, however, the others all employed one-dimensional GC-MS systems.
49
50
51
52
53
54
55
56
57
58
59
60

339 Considering all these different factors, a comparison of the molecules from this study with others
340 is challenging.

341 However, in an effort to translate this work to others, a remark on the overlap between the
342 molecules detected in the present and those reported in previous studies is provided. Eight
343 molecules detected in mouse breath were previously reported in the breath of infected non-
344 human primates and cows. Four molecules (tridecane, 2-heptanone, acetic acid phenyl ester and
345 *o*-cymene) were detected in the breath of non-human primates and reported as discriminatory
346 and statistically different between healthy and infected [21]; and four other molecules (styrene,
347 benzaldehyde, acetophenone, and nonanal) were reported in the breath of cows [19,20]. In the
348 present study, these molecules were not a part of the discriminatory feature set and they were not
349 statistically different between infected and control mice.










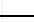
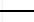
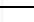







350 Human breath studies [12,14,18] cumulatively reported on 48 molecules, that discriminated
351 between patients whose sputum cultures were positive or negative for mycobacteria.

352 In the present study, four of the 48 (3-methylheptane, ethylbenzene, 4-methyldecane, and
353 acetaldehyde) were detected in mice breath and result discriminatory (**Table 2**). Acetaldehyde
354 was detected at a higher abundance in the mice infected with *M. bovis* BCG while 3-
355 methylheptane, ethylbenzene, and 4-methyldecane were in higher abundance in the PBS group.
356 Nine other molecules from the aforementioned human studies (4,6,8-trimethyl-1-nonene,
357 tridecane, octanal, 1,3-dimethyl-cyclohexane, camphene, heptanal, nonanal, 2-methylpentane,
358 styrene) were also detected in the breath of mice in the present contribution, however, none of
359 these molecules were discriminatory or statistically different between groups.

360 A comparison with volatile molecules from mycobacterial culture [35,36] is even more
361 complicated, due to differences in the sampling technique (*i.e.* SPME or NTME vs TD), and

1
2
3 362 heterogeneity of the biological conditions (*i.e.* different species of mycobacteria, *in vitro* vs *in*
4
5 363 *vivo* environment *etc.*).
6
7
8 364
9
10 365
11
12 366
13
14 367
15
16 368
17
18 369
19
20 370
21
22 371
23
24 372
25
26 373
27
28 374
29
30 375
31
32 376
33
34 377
35
36 378
37
38 379
39
40 380
41
42 381
43
44 382
45
46 383
47
48 384
49
50
51
52
53
54
55
56
57
58
59
60

385 **Table 2.** Tentative peak identification of the discriminatory molecules selected by random forest,
 386 formula, and relative abundance between the control and infected mice groups.

Peak no.	Tentative compound ID	Formula	Log ₂ (Control/Infected)
1	decyl-cyclohexane*	C ₁₆ H ₃₂	
2	methanethiol	CH ₄ S	
3	3,4-diethyl-2-hexene	C ₁₀ H ₂₀	
4	dimethyl sulphite	C ₂ H ₆ O ₃ S	
5	2,2,4,4-tetramethyl-3-pentanone	C ₉ H ₁₈ O	
6	acetaldehyde	C ₂ H ₄ O	
7	acetone	C ₃ H ₆ O	
8	2-butene	C ₄ H ₈	
9	3-oxo cyclopenten-1-yl-(2E)-penta-2,4-dienoate	C ₁₀ H ₁₀ O ₃	
10	4-methyl-decane	C ₁₁ H ₂₄	
11	ethylbenzene	C ₈ H ₁₀	
12	2,4,4-trimethyl-1-pentene	C ₈ H ₁₆	
13	4-methylene-1-(1-methylethyl)-bicyclo[3.1.0]hexane	C ₁₀ H ₁₆	
14	2-methyl-(E)-2-butenal	C ₅ H ₈ O	
15	2-ethyl-3-methylbutanal	C ₇ H ₁₄ O	
16	2-methylheptane	C ₈ H ₁₈	
17	butanal	C ₄ H ₈ O	
18	3-methylheptane	C ₈ H ₁₈	
19	(2-aziridinyloethyl)amine	C ₄ H ₁₀ N ₂	
20	3-methyl-(Z)-4-nonene	C ₁₀ H ₂₀	Driving room air separation
21	2-decen-1-ol	C ₁₀ H ₂₀ O	Driving room air separation
22	4-[2-(methylamino)ethyl]-phenol	C ₁₀ H ₁₅ NO ₂	Driving room air separation
23	3,4-dimethylpentanol	C ₇ H ₁₆ O	Driving room air separation

-4 -2 0 +2 +4

387 *Feature statistically different between infected and control mouse groups ($p < 0.05$).

 Infected
 Control

388 **Conclusions and future perspectives**

389 Breath holds great potential as a carrier of information on the health status of an individual and
390 animal models are important tools in the quest to better diagnose and understand infectious
391 diseases.

392 In this study, breath was collected for the first time from mice infected with an MTBC pathogen,
393 *M. bovis* BCG, and contrasted with breath from animals instilled with PBS. The immunological
394 and bacterial cell count data at the time of breath collection confirmed the infection status of the
395 animals treated with the pathogen. From the entire spectrum of volatile metabolites in breath,
396 twenty-three molecules were tentatively identified and selected as a panel that could distinguish
397 between infected and uninfected animals. Four of them are in common with the possible
398 biomarkers reported in previous studies on breath from animals with an MTBC infection.

399 The information obtained in this study can be used to further develop a mouse breath model for
400 MTBC lung infections as potential diagnostic or drugs treatment monitoring approach, as well as
401 a tool for a better understanding of disease pathogenesis by volatile metabolites expression.
402 Future studies will focus on establishing links between the metabolites and their associated
403 pathogen and/or host pathways.

405 **Acknowledgements**

406 The authors would like to thank Emily M. Nakada, Ph.D. (University of Vermont) for assisting
407 with flow cytometry. We thank Mavra Nasir and Chris Rees for their aid in editing this
408 manuscript. This work was supported by the Bill and Melinda Gates Foundation (OPP1135516).

410

411 **References**

- 412 [1] Adams F 1994 Hippocratic Writings *Hippocratic Writings: Aphorism 4,5* (New York:
413 Web Atomics) p Aphorism 4,5
- 414 [2] Pauling L, Robinson A B, Teranishi R and Cary P 1971 Quantitative Analysis of Urine
415 Vapor and Breath by Gas-Liquid Partition Chromatography *Proc. Natl. Acad. Sci.* **68**
416 2374–6
- 417 [3] Boots A W, Joep J B N van B, Jan W D, Agnieszka S, Emile F W and Frederik J van S
418 2012 The versatile use of exhaled volatile organic compounds in human health and
419 disease *J. Breath Res.* **6** 27108
- 420 [4] de Lacy Costello B, Amann a, Al-Kateb H, Flynn C, Filipiak W, Khalid T, Osborne D
421 and Ratcliffe N M 2014 A review of the volatiles from the healthy human body. *J. Breath*
422 *Res.* **8** 14001
- 423 [5] Gruber B, Keller S, Groeger T, Matuschek G, Szymczak W and Zimmermann R 2016
424 Breath gas monitoring during a glucose challenge by a combined PTR-QMS/GC×GC-
425 TOFMS approach for the verification of potential volatile biomarkers *J. Breath Res.* **10**
426 36003
- 427 [6] Capuano R, Santonico M, Pennazza G, Ghezzi S, Martinelli E, Roscioni C, Lucantoni G,
428 Galluccio G, Paolesse R, Di Natale C and D'Amico A 2015 The lung cancer breath
429 signature: a comparative analysis of exhaled breath and air sampled from inside the lungs
430 *Sci. Rep.* **5** 16491
- 431 [7] Fens N, Zwinderman A H, Van Der Schee M P, De Nijs S B, Dijkers E, Roldaan A C,
432 Cheung D, Bel E H and Sterk P J 2009 Exhaled breath profiling enables discrimination of
433 chronic obstructive pulmonary disease and asthma *Am. J. Respir. Crit. Care Med.* **180**

- 1
2
3 434 1076–82
4
5 435 [8] Filipiak W, Beer R, Sponring A, Filipiak A, Ager C, Schiefecker A, Lanthaler S, Helbok
6
7 R, Nagl M, Troppmair J and Amann A 2015 Breath analysis for *in vivo* detection of
8 436
9 pathogens related to ventilator-associated pneumonia in intensive care patients: a
10 437
11 prospective pilot study *J. Breath Res.* **9** 16004
12 438
13
14 439 [9] Connie R. Mahon, Donald C. Lehman G M J 2008 *Textbook of Diagnostic Microbiology*
15
16 ed E H Sciences
17 440
18
19 441 [10] WHO 2016 *WHO | Global tuberculosis report 2016*
20
21 442 [11] Rodriguez-Campos S, Smith N H, Boniotti M B and Aranaz A 2014 Overview and
22
23 phylogeny of Mycobacterium tuberculosis complex organisms: Implications for
24 443
25 diagnostics and legislation of bovine tuberculosis *Res. Vet. Sci.*
26 444
27
28 445 [12] Phillips M, Cataneo R N, Condos R, Ring Erickson G A, Greenberg J, La Bombardi V,
29
30 Munawar M I and Tietje O 2007 Volatile biomarkers of pulmonary tuberculosis in the
31 446
32 breath *Tuberculosis* **87** 44–52
33 447
34
35 448 [13] Phillips M, Basa-Dalay V, Blais J, Bothamley G, Chaturvedi A, Modi K D, Pandya M,
36
37 Natividad M P R, Patel U, Ramraje N N, Schmitt P and Udwardia Z F 2012 Point-of-care
38 449
39 breath test for biomarkers of active pulmonary tuberculosis *Tuberculosis* **92** 314–20
40 450
41
42 451 [14] Phillips M, Basa-Dalay V, Bothamley G, Cataneo R N, Lam P K, Natividad M P R,
43
44 Schmitt P and Wai J 2010 Breath biomarkers of active pulmonary tuberculosis
45 452
46
47 453 *Tuberculosis* **90** 145–51
48
49 454 [15] Sahota A S, Gowda R, Arasaradnam R P, Daulton E, Savage R S, Skinner J R, Adams E,
50
51 Ward S A and Covington J A 2016 A simple breath test for tuberculosis using ion
52 455
53 mobility: A pilot study *Tuberculosis* **99** 143–6
54 456
55
56
57
58
59
60

- 1
2
3 457 [16] Soobratty M R, Whitfield R, Subramaniam K, Grove G, Carver A, O'Donovan G V., Wu
4
5 458 H H T, Lee O Y C, Swaminathan R, Cope G F and Milburn H J 2014 Detecting active
6
7 459 pulmonary tuberculosis with a breath test using nanomaterialbased sensors *Eur. Respir. J.*
8
9 460 **43** 1519–22
- 11
12 461 [17] Bruins M, Rahim Z, Bos A, Van De Sande W W J, Endtz H P and Van Belkum A 2013
13
14 462 Diagnosis of active tuberculosis by e-nose analysis of exhaled air *Tuberculosis* **93** 232–8
- 16
17 463 [18] Kolk A H J, van Berkel J J B N, Claassens M M, Walters E, Kuijper S, Dallinga J W and
18
19 464 van Schooten F J 2012 Breath analysis as a potential diagnostic tool for tuberculosis. *Int.*
20
21 465 *J. Tuberc. lung Dis. Off. J. Int. Union against Tuberc. Lung Dis.* **16** 777–82
- 23
24 466 [19] Peled N, Ionescu R, Nol P, Barash O, McCollum M, Vercauteren K, Koslow M, Stahl R,
25
26 467 Rhyan J and Haick H 2012 Detection of volatile organic compounds in cattle naturally
27
28 468 infected with *Mycobacterium bovis* *Sensors Actuators, B Chem.* **171–172** 588–94
- 30
31 469 [20] Ellis C K, Stahl R S, Nol P, Waters W R, Palmer M V., Rhyan J C, VerCauteren K C,
32
33 470 McCollum M and Salman M D 2014 A pilot study exploring the use of breath analysis to
34
35 471 differentiate healthy cattle from cattle experimentally infected with *Mycobacterium bovis*
36
37 472 *PLoS One* **9**
- 39
40 473 [21] Mellors T R, Blanchet L, Flynn J L, Tomko J, O'Malley M, Scanga C A, Lin P L and Hill
41
42 474 J E 2017 A new method to evaluate macaque health using exhaled breath: A case study of
43
44 475 *M. tuberculosis* in a BSL-3 setting *J. Appl. Physiol.* jap.00888.2016
- 46
47 476 [22] Flynn J L 2006 Lessons from experimental *Mycobacterium tuberculosis* infections **8**
- 48
49 477 [23] Tranchida P Q, Franchina F A, Dugo P and Mondello L 2016 Comprehensive two-
50
51 478 dimensional gas chromatography-mass spectrometry: Recent evolution and current trends
52
53 479 *Mass Spectrom. Rev.* **35**
- 55
56
57
58
59
60

- 1
2
3 480 [24] Zhu J, Jimenez-Diaz J, Bean H D, Daphtary N A, Aliyeva M I, Lundblad L K A and Hill
4
5 481 J E 2013 Robust detection of *P. aeruginosa* and *S. aureus* acute lung infections by
6
7 482 secondary electrospray ionization-mass spectrometry (SESI-MS) breathprinting: from
8
9 483 initial infection to clearance. *J. Breath Res.*
- 11
12 484 [25] Dieterle F, Ross A, Schlotterbeck G and Senn H 2006 Probabilistic quotient
13
14 485 normalization as robust method to account for dilution of complex biological mixtures.
15
16 486 Application in ¹H NMR metabonomics *Anal. Chem.*
- 18
19 487 [26] Hastie T, Tibshirani R and Friedman J 2009 The Elements of Statistical Learning *The*
20
21 488 *Elements of Statistical Learning*
- 23
24 489 [27] Li S, Aliyeva M, Daphtary N, Martin R a., Poynter M E, Kostin S F, van der Velden J L,
25
26 490 Hyman A M, Stevenson C S, Phillips J E and Lundblad L K a. 2014 Antigen-induced
27
28 491 mast cell expansion and bronchoconstriction in a mouse model of asthma *AJP Lung Cell.*
29
30 492 *Mol. Physiol.*
- 32
33 493 [28] Balamayooran G, Batra S, Fessler M B, Happel K I and Jeyaseelan S 2010 Mechanisms
34
35 494 of neutrophil accumulation in the lungs against bacteria *Am. J. Respir. Cell Mol. Biol.* **43**
36
37 495 5–16
- 39
40 496 [29] Bean H D, Jiménez-Díaz J, Zhu J and Hill J E 2015 Breathprints of model murine
41
42 497 bacterial lung infections are linked with immune response *Eur. Respir. J.*
- 44
45 498 [30] Lombard R, Doz E, Carreras F, Eparaud M, Le Vern Y, Buzoni-Gatel D and Winter N
46
47 499 2016 IL-17RA in non-hematopoietic cells controls CXCL-1 and 5 critical to recruit
48
49 500 neutrophils to the lung of mycobacteria-infected mice during the adaptive immune
50
51 501 response *PLoS One* **11**
- 53
54 502 [31] Schreiber O, Steinwede K, Ding N, Srivastava M, Maus R, Länger F, Prokein J, Ehlers S,
55
56
57
58
59
60

1
2
3 503 Welte T, Gunn M D and Maus U a 2008 Mice that overexpress CC chemokine ligand 2 in
4
5 504 their lungs show increased protective immunity to infection with *Mycobacterium bovis*
6
7
8 505 bacille Calmette-Guérin. *J. Infect. Dis.*

9
10 506 [32] Srivastava M, Meinders A, Steinwede K, Maus R, Lucke N, Bühling F, Ehlers S, Welte T
11
12 507 and Maus U A 2007 Mediator responses of alveolar macrophages and kinetics of
13
14 508 mononuclear phagocyte subset recruitment during acute primary and secondary
15
16 509 mycobacterial infections in the lungs of mice *Cell. Microbiol.*

17
18
19 510 [33] Ghimenti S, Lomonaco T, Bellagambi F G, Tabucchi S, Onor M, Trivella M G, Ceccarini
20
21 511 A, Fuoco R and Di Francesco F 2015 Comparison of sampling bags for the analysis of
22
23 512 volatile organic compounds in breath *J. Breath Res.*

24
25
26 513 [34] Hinkle D E, Wiersma W and Jurs S G 2003 *Applied Statistics for the Behavioral Sciences*
27
28 514 (Houghton Mifflin)

29
30 515 [35] Küntzel A, Fischer S, Bergmann A, Oertel P, Steffens M, Trefz P, Miekisch W, Schubert
31
32 516 J K, Reinhold P and Köhler H 2016 Effects of biological and methodological factors on
33
34 517 volatile organic compound patterns during cultural growth of *Mycobacterium avium* ssp .
35
36 518 *paratuberculosis* *J. Breath Res.*

37
38
39 519 [36] Mellors T R, Rees C A, Wieland-Alter W F, von Reyn C F and Hill J E 2017 The volatile
40
41 520 molecule signature of four mycobacteria species *J. Breath Res.* **11** 31002

42
43
44 521

45
46
47 522

48
49
50

51
52
53

54
55
56

57
58
59

60